Mathematics in Industry 17
The European Consortium for Mathematics in Industry

Michael Günther
Andreas Bartel
Markus Brunk
Sebastian Schöps
Michael Striebel *Editors*

Progress in Industrial Mathematics at ECMI 2010

Springer

MATHEMATICS IN INDUSTRY 17

THE EUROPEAN CONSORTIUM
FOR MATHEMATICS IN INDUSTRY

For further volumes:
http://www.springer.com/series/4650

Michael Günther
Andreas Bartel
Markus Brunk
Sebastian Schöps
Michael Striebel
Editors

Progress in Industrial Mathematics at ECMI 2010

With 194 Figures, 71 in color and 26 Tables

Springer

Editors
Michael Günther
University of Wuppertal
Wuppertal
Germany

Andreas Bartel
University of Wuppertal
Wuppertal
Germany

Markus Brunk
Robert Bosch GmbH
Stuttgart
Germany

Sebastian Schöps
University of Wuppertal
Wuppertal
Germany

Michael Striebel
University of Wuppertal
Wuppertal
Germany

ISBN 978-3-642-25099-6 e-ISBN 978-3-642-25100-9
DOI 10.1007/978-3-642-25100-9
Springer Heidelberg Dordrecht London New York

Library of Congress Control Number: 2012933374

Mathematics Subject Classification (2010): 34, 35, 49, 60, 62, 65, 68, 70, 74, 76, 87, 80, 81, 86, 91, 92, 94

Preface

The 16th conference of the European Consortium for Mathematics in Industry took place in the *Historische Stadthalle Wuppertal*, the historical city hall of Wuppertal, Germany, from July 26 to July 30, 2010. This venue, a member of the Historic Conference Centers of Europe, is one of the most remarkable concert halls and conference centers in Europe.

The organizers welcomed nearly 250 registered participants from 30 different countries. Most of the participants contributed actively to the scientific program of the conference, which included—besides a poster session accompanied by an extended coffee break sponsored by ST Microelectronics—10 plenary talks, 132 talks within 27 minisymposia and 57 contributed talks. In this proceedings, industrial mathematics appears in a wide range of applications and methods, reflecting the topics addressed at ECMI 2010: from Circuit and Electromagnetic Device Simulation, Model Order Reduction for Chip Design, Uncertainties and Stochastics, Production, Fluids, Life and Environmental Sciences to Dedicated and Versatile Methods. We should mention that of the 106 contributions that were submitted to these proceedings, 76 have been selected for publication after a peer review process.

We would like to recall some of the highlights of our conference: On Monday evening, the public lecture *Modern Mathematics for Better Technologies* was given by Volker Mehrmann, president of Matheon. He emphasized mathematics as an innovation enabler for industry and business, and as an absolutely essential prerequisite for Europe on its way to becoming the leading knowledge-based economy in the world. The same day, Volker Mehrmann chaired a panel discussion to promote and facilitate this process based on the outcome and recommendations of the Forward Look Project *Mathematics and Industry* of the European Science Foundation.

On Wednesday, the *Associazione Angelo Marcello Anile* and ECMI together awarded the first Anile-ECMI Prize for Mathematics in Industry, which is dedicated to young researchers for excellent PhD theses in industrial mathematics. It was initiated to honor the memory of the former ECMI council member Angelo Marcello Anile (1948–2007), Professor of Applied Mathematics at the University of Catania,

Photograph: Sebastian Jarych.

Italy. This prize was awarded to Andriy Vasyliovich Hlod for his PhD thesis at TU Eindhoven, The Netherlands. It included an invited talk, which he gave on *Jets of Viscous Fluid*. Continuing a long tradition of the ECMI conferences and following the suggestion of the Local Organizing Committee, honorary membership of ECMI was awarded to Willi Jäger, Professor of Applied Mathematics and founder of the IWR at the University of Heidelberg, for his pioneering work in Applied and Industrial Mathematics. The award ceremony took place during the conference dinner in the large ballroom of the historical city hall, a magnificent example of the art nouveau style of architecture.

ECMI 2010 would never have been the success it was without the help of many. Among them, first of all, the participants, the speakers and the Program Committee. We thank Lambert T. Koch, Rector of the *Bergische Universität Wuppertal*, whose negotiation skills—together with the gratefully acknowledged financial support of all our sponsors and partners (see: `www.ecmi2010.eu`)—allowed us to select for the conference the unique venue of ECMI 2010, the *Historische Stadthalle Wuppertal* for nearly 1 week. Special thanks go to our team assistants Elvira Mertens, Lisa Hartmann and Eva Winnemöller for their excellent administrative support. We are very grateful to our colleagues Matthias Ehrhardt and Roland Pulch for their invaluable work within the local organizing committee. Finally we would like to acknowledge the great support of the many students who helped us during the conference, e.g., by setting up the equipment and answering technical and practical questions.

Wuppertal and Stuttgart
Germany

Michael Günther
Andreas Bartel
Markus Brunk
Sebastian Schöps
Michael Striebel

Contents

Part I
Circuit and Electromagnetic Device Simulation

Overview

Today's electric and electronic industries rely heavily on computer aided engineering tools. The high complexity of devices and the increasing speed of innovation cycles necessitate virtual prototyping. This allows such production at a competitive time to market because virtual experiments are faster and cheaper than their physical ancestors. Thus numerical tools for those simulations play a key role in the electrical engineering industry. Commonly, the underlying principles from physics are well established but the simulation techniques are still a topic of ongoing research, e.g. due to new computational possibilities stemming from advances in computer architectures. The research focuses in particular on improving the general efficiency and robustness of simulations (more accurate results in less time) and the interaction/coupling of multiphysical problems (secondary effects cannot be disregarded anymore).

In particular electronic industry relies on efficient numerical experiments of their new designs, e.g., layouts for printed circuit boards. The corresponding circuits result from combining smaller subcircuits. One of the most common configurations is the oscillator, i.e., an electronic device that creates a repetitive signal. Owing to the large number of such devices and their nonlinearity often computational expensive time-domain simulations are necessary. New efficient methods are needed to validate the designs in a reasonable time. To this end K. Bittner and E. Dautbegovic propose in '*Wavelet Algorithm for Circuit Simulation*' the usage of wavelets in circuit simulation. The authors present a new algorithm based on spline wavelets. The unknowns are expanded into a wavelet representation, which is determined as a solution to nonlinear equations derived from the circuit equations by a Galerkin discretization. Applications, e.g. an oscillator, show that for the same accuracy fewer grid points are needed compared to standard transient analysis.

The structural aspects of circuit configurations with oscillations are analyzed by R. Riaza and C. Tischendorf in '*Structural Characterization of Circuit Configurations with Undamped Oscillations*'. Undamped oscillations in linear circuits arise

from the existence of purely imaginary eigenvalues in the matrix pencil spectrum. The authors investigate the corresponding circuit configurations based on branch-oriented circuit models and on several results from digraph theory.

H.G. Brachtendorf and R. Laur study in '*Entrainment Phenomena in Nonlinear Oscillations*' entrainment phenomena in nonlinear oscillations in particular for devices that mix down a radio frequency signal to an intermediate frequency (IF). Circuit designs have been developed using injection locking for the design, but unwanted temporary entrainment known as "pulling" can be a severe cause of performance degradation for zero-IF or low-IF transceivers. The corresponding entrainment effects have been studied for decades. The authors develop a new theory based on a perturbation technique employing Floquet's theory.

On the other hand, when analyzing oscillators in the frequency domain, the simulation often suffers from poor initial conditions. Hence J. Virtanen et al. propose in '*Initial Conditions and Robust Newton-Raphson for Harmonic Balance Analysis of Free-Running Oscillators*' to use time integration to obtain estimates for the oscillation frequency and for the oscillator solution. They also describe new techniques from bordered matrices and eigenvalue methods to improve Newton methods for finite difference techniques in the time domain as well as for Harmonic Balance.

The classical network approach is not sufficient if complex devices must be taken into account and lumped device models are not available. Then the extraction of macromodels by using tabulated S-parameter frequency responses allows us to synthesize SPICE compatible models. In '*Rational Modeling Algorithm for Passive Microwave Structures and Systems*' D. Deschrijver et al. discuss a method that constructs such macromodels which are passive by construction. The authors apply a new passivity enforcement technique that is able to guarantee passivity by means of an overdetermined least-squares fitting algorithm.

In contrast, if the simulation engineer is interested in both the macroscopic behavior of the circuit and additionally in the microscopic phenomena inside of a particular device, then only a full coupled simulation is the way out. G. Alì et al. discuss in '*An Existence Result for Index-2 PDAE System Arising in Semiconductor Modeling*' the existence of solutions for the case of an electric network containing semiconductor devices. The coupled system consists of the Modified Nodal Analysis equations with multi-dimensional elliptic partial differential equations modeling the devices (drift diffusion model).

The microscopic behavior of charge carriers in semiconductors is described more accurately by the solution of the Boltzmann transport equation (BTE). However, the Monte-Carlo method, preferably used for solving the BTE suffers from intense numerical complexity. A numerically less expensive approach is presented by K. Rupp et al. in '*Deterministic Numerical Solution of the Boltzmann Transport Equation*'. They consider the deterministic numerical solution of the Boltzmann transport equation and present the deterministic Spherical Harmonic Expansion (SHE) method for the determination of the solution of the BTE. The solution of the SHE-model faces the problem of intense memory consumption. However, the

authors present a new lossless system matrix compression scheme which allows for a significant reduction of memory consumption.

Due to increasing complexity and ongoing miniaturization in the layout and production of semiconductor devices, forecasting of thermal effects and prediction of hotspots has become more and more important within the last years and compels us to develop more reliable models. This subject has been addressed by several authors during the ECMI 2010. In '*Analysis of Self-Heating Effects in Sub-Micron Silicon Devices with Electrothermal Monte Carlo Simulations*' O. Muscato and V. Di Stefano solve the BTE with a thermal model by a Monte-Carlo method, coupled to a Cattaneo-like equation for the lattice temperature, which is obtained in the framework of extended irreversible thermodynamics.

G. Alì et al. on the other hand present a new macroscopic energy-transport model incorporating thermal effects in the crystal lattice of the semiconductors. This is done by considering the diffusive limit of MEP hydrodynamical model obtained from the Bloch-Boltzmann-Peierls equation for semiconductors in '*Diffusive Limit of a MEP Hydrodynamical Model Obtained from the Bloch-Boltzmann-Peierls Equations for Semiconductors*'. Thereby, the authors introduce a smallness parameter related to the transition probabilities in the collision operators and a diffuse scaling at the level of the Lagrangian multipliers that appear in the closure relations. Based on this procedure, the authors obtain a system of model equations, which include energy-transport equations that are consistent with the linear irreversible thermodynamics.

G. Greco and S. Rinaudo give us some insight into the application of semiconductor device simulation at ST Microelectronics in Catania and present automatic layout optimization of power discrete devices using innovative distributed model techniques, '*Automatic Layout Optimization of Power Discrete Devices Using Innovative Distributed Model Techniques*'. The increasing usage of power MOSFETs in application enforces an optimization of the geometry. This is essential for the reduction of hotspots. Since microscopic models are too costly to simulate in an optimization loop, a distributed model technique is described where the device is divided into several cells connected e.g. by transmission lines. This distributed approach is embedded into an optimization algorithm in order to optimize geometry.

A. El Boukili presents 3D stress simulations of nano transistors, '*3D Stress Simulations of Nano Transistors*'. Mechanical stress is intentionally used by semiconductor manufacturers to optimize the performance of devices. This requires semiconductor models to incorporate these effects. The author extends three dimensional semiconductor model equations by coupling them with a mechanical stress model from linear elasticity theory. Based on his simulation results he proposes the modification of existing mobility results and gives interesting ideas in this direction.

On the macroscopic level, many devices can be represented by Maxwell's equations. They describe the spatial distribution of the electromagnetic field by partial differential equations. Simulations follow typically the method of lines: the equations are restated in a more compact formulation (e.g. using the magnetic vector potential as its unknown) and then discretized in space. Finally the resulting system is solved in the time domain.

In '*Hybrid Formulations and Discretisations for Magnetoquasistatic Models*' H. De Gersem et al. propose the usage of hybrid formulations and discretizations for the magnetoquasistatic approximation of Maxwell's equations. This increases the modeling flexibility because distinct model regions can be tackled by different approaches. The authors explain in detail which algebraic solution techniques are necessary for solving the coupled systems of equations and demonstrate their approach using numerical examples.

G. Ala et al. diverge from the standard discretization procedures and propose in '*A 3D Meshless Approach for Transient Electromagnetic PDE*' a new meshless approach for the Maxwell's 3D full wave equation. They employ the smoothed particle hydrodynamic method by considering the particles as interpolation points, arbitrarily placed in the computational domain. Simulations validate the method and allow a comparison with standard approaches, i.e., the finite difference time domain method.

The final contribution to this chapter, '*Modelling and Analysis of the Nonlinear Dynamics of the Transrapid and Its Guideway*', focusses on a coupled simulation of a real-world industrial example: the Transrapid and its guideway. M. Dellnitz et al. couple the mechanical and electromagnetic parts, i.e., the control subsystems, magnet subsystems, a lateral cross-section and a vertical dynamics model as a multibody system. It is verified using simulations, eigenmode analysis and displacement measurements from train passages on a test track. They show that ground vibrations caused by the vehicle can be significantly reduced by a flexible spring-mass system as a support for the girders.

Wuppertal and Stuttgart, Germany

Sebastian Schöps
Markus Brunk

Wavelet Algorithm for Circuit Simulation

Kai Bittner and Emira Dautbegovic

Abstract We present a new adaptive circuit simulation algorithm based on spline wavelets. The unknown voltages and currents are expanded into a wavelet representation, which is determined as solution of nonlinear equations derived from the circuit equations by a Galerkin discretization. The spline wavelet representation is adaptively refined during the Newton iteration. The resulting approximation requires an almost minimal number of degrees of freedom, and in addition the grid refinement approach enables very efficient numerical computations. Initial numerical tests on various types of electronic circuits show promising results when compared to the standard transient analysis.

1 Introduction

Wavelet theory emerged during the twentieth century from the study of Calderon-Zygmund operators in mathematics, the study of the theory of subband coding in engineering and the study of renormalization group theory in physics. Recent approaches [1, 4, 7–9] to the problem of multirate envelope simulation indicate that wavelets could also be used to address the qualitative simulation challenge by a development of novel wavelet-based circuit simulation techniques capable of an efficient simulation of a mixed analog-digital circuit [6].

K. Bittner (✉)
University of Wuppertal, Gaußstraße 20, 42119 Wuppertal, Germany
e-mail: bittner@math.uni-wuppertal.de

E. Dautbegovic
Infineon Technologies AG, 81726 Munich, Germany
e-mail: Emira.Dautbegovic@infineon.com

M. Günther et al. (eds.), *Progress in Industrial Mathematics at ECMI 2010*,
Mathematics in Industry 17, DOI 10.1007/978-3-642-25100-9_1,

The wavelet expansion of a function f is given as

$$f = \sum_{k \in \mathscr{I}} c_k \, \phi_k + \sum_{j=0}^{\infty} \sum_{k \in \mathscr{K}_j} d_{jk} \, \psi_{jk}. \tag{1}$$

Here, j refers to a level of resolution, while k describes the localization in time or space, i.e., ψ_{jk} is essentially supported in the neighborhood of a point x_{jk} of the domain, where the wavelet expansion is defined. The wavelet expansion can be seen as coarse scale approximation $\sum_{k \in \mathscr{I}} c_k \, \phi_k$ by the scaling functions ϕ_k complemented by information on details of increasing resolution j in terms of the wavelets ψ_{jk}. Since a wavelet basis consist of an infinite number of wavelets one has to consider approximations of f by partial sums of the wavelet expansion (1), which can, e.g., be obtained by ignoring small coefficients.

2 Wavelet-Based Galerkin Method

We consider circuit equations in the charge/flux oriented modified nodal analysis (MNA) formulation, which yields a mathematical model in the form of an initial-value problem of differential-algebraic equations (DAEs):

$$\frac{d}{dt}\mathbf{q}\big(\mathbf{x}(t)\big) + \mathbf{f}\big(\mathbf{x}(t)\big) = \mathbf{s}(t). \tag{2}$$

Here $\mathbf{x}$ is the vector of node potentials and specific branch voltages and $\mathbf{q}$ is the vector of charges and fluxes. Vector $\mathbf{f}$ comprises static contributions, while $\mathbf{s}$ contains the contributions of independent sources.

In our adaptive wavelet approach we first discretize the MNA equation (2) in terms of the wavelet basis functions, by expanding $\mathbf{x}$ as a linear combination of wavelets or related basis functions φ_i, i.e., $\mathbf{x} = \sum_{i=0}^{n} \mathbf{c}_i \, \varphi_i$. Furthermore, we integrate the circuit equations against test functions θ_ℓ and obtain the equations

$$\int_0^T \Big(\frac{d}{dt}\mathbf{q}\big(\mathbf{x}(t)\big) + \mathbf{f}\big(\mathbf{x}(t)\big) - \mathbf{s}(t) \Big) \, \theta_\ell \, dt = 0, \tag{3}$$

for $\ell = 1, \ldots, n$. Together with the initial conditions $\mathbf{x}(0) = \mathbf{x}_0$, we have now $n+1$ vector valued equations, which determine the coefficients $\mathbf{c}_i$ provided that the test functions θ_ℓ are chosen suitably to the basis functions φ_i.

The nonlinear system (3) is solved by Newton's method. With a good initial guess, Newton's method is known to converge quadratically. Unfortunately, a good initial guess is usually not available, and convergence can often only be obtained after a large number of (possibly damped) Newton steps. On the other hand, to get a good approximation of the solution of (2), the space $X = \operatorname{span}\{\varphi_k : \ k = 0, \ldots, n\}$ has to be sufficiently large and the computational cost of each step depends on $n = \dim X$.

Here, we take advantage from the use of wavelets. The Newton iteration is started on a coarse subspace X_0 of small dimension, which provides us with a first coarse approximation $x^{(0)}$ of the solution. Then $x^{(0)}$ is used as initial guess for a Newton iteration in a finer space $X_1 \supset X_0$, leading to an improved approximation $x^{(1)}$. One positive effect, which can be observed in numerical tests, is that a single Newton step in the beginning of the algorithm is relatively cheap, i.e., having only a poor initial guess for $x^{(i)}$ with i small has only a negligible effect on the performance of the algorithm. On the other hand, due to the excellent initial guess in the higher dimensional spaces X_i with i large, we need only a few of the costly Newton steps, which are necessary in order to achieve a required accuracy. The embedding $X_i \subset X_{i+1}$ is ensured by the use of wavelet subsets, i.e.,

$$X_i = \operatorname{span}\Big(\{\phi_k : k \in \mathscr{I}\} \cup \{\psi_{jk} : (j,k) \in \Lambda_i\}\Big), \qquad \Lambda_i \subset \Lambda_{i+1},$$

i.e., we add adaptively more and more wavelets to the expansion.

Due to the intrinsic properties of wavelets [6] an adaptive wavelet approximation can provide an efficient representation of functions with steep transients, which often appear in a mixed analog/digital electronic circuit. However, for an efficient circuit simulation we have to take further properties of a wavelet system into account. We consider spline wavelets to be the optimal choice since spline wavelets are the only wavelets with an explicit formulation. This permits the fast computation of function values, derivatives and integrals, which is essential for an efficient solution of a nonlinear problem as given in (2) (see also [3,5]). Spline wavelets have already been used for circuit simulation [10]. However, here we use a completely new approach based on spline wavelets from [2].

3 Numerical Tests

A prototype of the proposed wavelet algorithm is implemented within the framework of a productively used circuit simulator and tested on a variety of circuits. For all examples we have compared the CPU time and the grid size (i.e., the number of spline knots or time steps) with the corresponding results from transient analysis of the same circuit simulator.

The error is estimated by comparison with well-established and highly-accurate transient analysis. The estimate shown in the signal is the maximal absolute difference over all grid points of the transient analysis, which gives a good approximation of the maximal error. That is, if we can obtain a small error for the wavelet analysis, which proves good agreement with the standard method. In particular, since we compare the solutions of two independent methods we have very good evidence that we approximate the solution of the underlying DAE's with the estimated error.

3.1 Amplifier

The amplifier is simulated with a pulse signal of period 1 ns, which is modulated by a piecewise smooth amplitude (see Fig. 1). The wavelet method runs over 100 ns. The results show a satisfying performance also for digital-like input signals (Figs. 2 and 3).

3.2 Oscillator

The oscillator is an autonomous circuit without an external input signal. The simulation runs over 20 ns. As can be seen from Fig. 4, an excellent agreement with highly-accurate transient analysis is achieved. It should be noted that after the oscillator has reached its periodic steady state the wavelet method works very fast, since the solution from one interval is an excellent initial guess for the next interval.

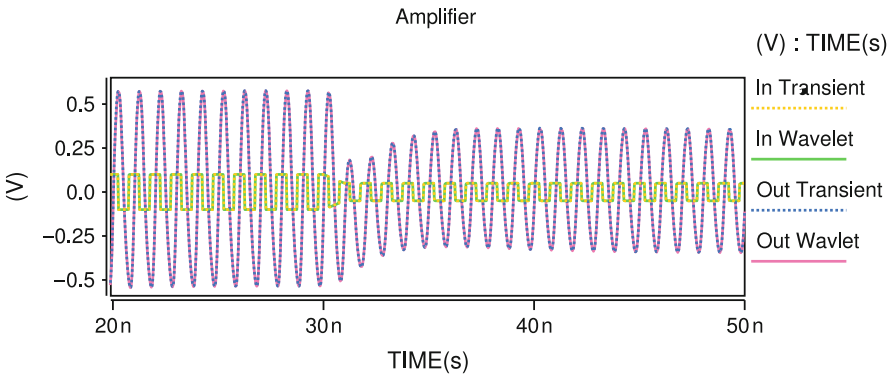

Fig. 1 Detail of input and output signal for the amplifier

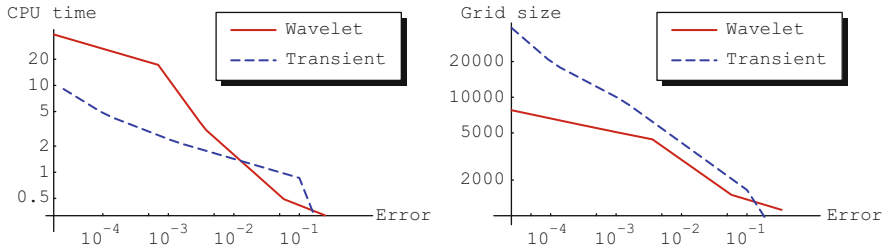

Fig. 2 Simulation statistics for the amplifier. Computation time versus error (*left*), and grid size versus error (*right*) for transient analysis and adaptive wavelet analysis

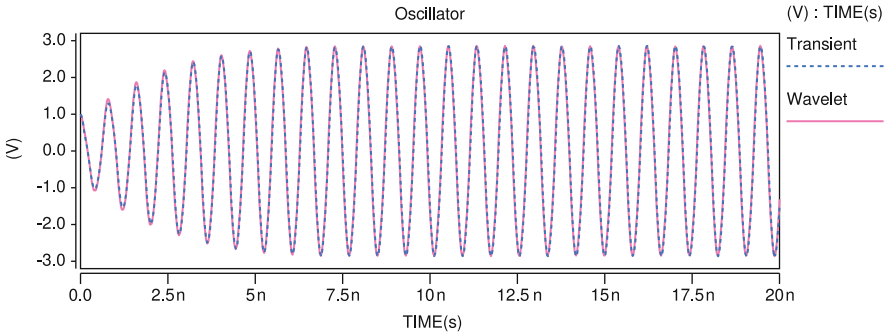

Fig. 3 Output signal for the oscillator

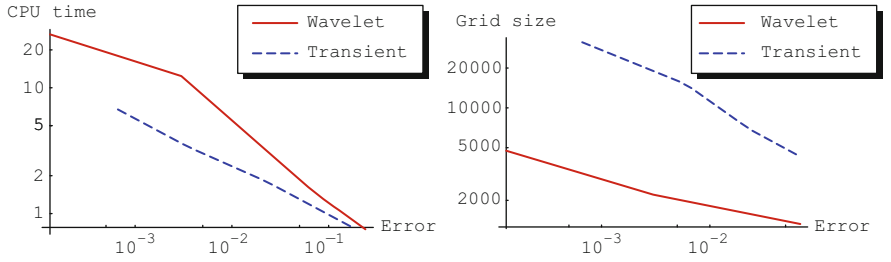

Fig. 4 Simulation statistics for the oscillator. Computation time versus error (*left*), and grid size versus error (*right*) for transient analysis and adaptive wavelet analysis

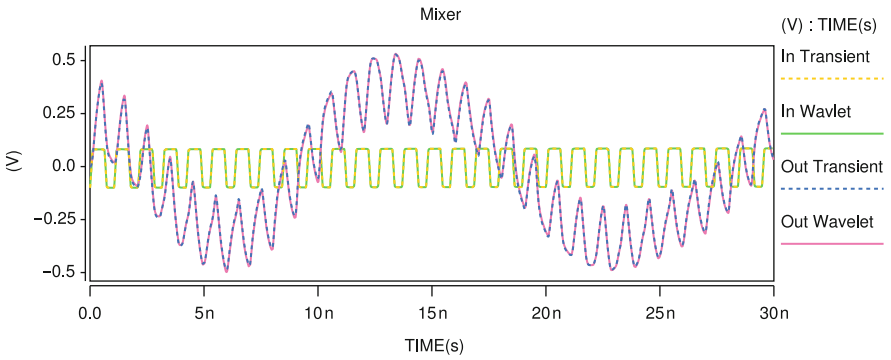

Fig. 5 Time domain input and output signal for the mixer

3.3 Mixer

The mixer is simulated with input frequencies 950 MHz and 1 GHz. The simulation runs over 30 ns. In particular, for high accuracies the number of degrees of freedom is essentially reduced, while the computation time is at least of the same order (Fig. 6).

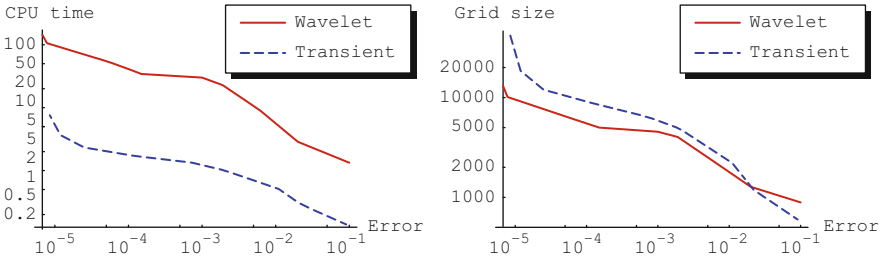

Fig. 6 Simulation statistics for the mixer. Computation time versus error (*left*), and grid size versus error (*right*) for transient analysis and adaptive wavelet analysis

4 Conclusion

The results of the simulations indicate that the wavelet based method may achieve and in some cases surpass performance of the standard transient analysis. Apparently, the number of degrees of freedom can be smaller than for the transient analysis for comparable accuracy. However, this advantage of the wavelet algorithm does not always result (yet) in a smaller computation time. On the other hand it can be expected that the productive implementation of the wavelet algorithm can be further optimized. Therefore our activities on optimization and further development of the wavelet-based algorithm are continuing.

Acknowledgements This work has been supported within the EU Seventh Research Framework Project (FP7) ICESTARS with the grant number 214911.

References

1. Barthel, A., Knorr, S., Pulch, R.: Wavelet based methods for multirate partial differential-algebraic equations. Appl. Numer. Math. **59**, 495–506 (2008)
2. Bittner, K.: Biorthogonal spline wavelets on the interval. In: Chen, G., Lai, M.J. (eds.) Wavelets and Splines: Athens 2005, pp. 93–104. Nashboro Press, Brentwood (2006)
3. Bittner, K., Urban, K.: Adaptive wavelet methods using semiorthogonal spline wavelets: Sparse evaluation of nonlinear functions. Appl. Comput. Harmon. Anal. **24**, 94–119 (2008)
4. Christoffersen, C., Steer, M.: State-variable-based transient circuit simulation using wavelets. IEEE Microw. Wireless Compon. Lett. **11**, 161–163 (2001)
5. Dahmen, W., Schneider, R., Xu, Y.: Nonlinear functionals of wavelet expansions — adaptive reconstruction and fast evaluation. Numer. Math. **86**, 49–101 (2000)
6. Dautbegovic, E.: Wavelets in circuit simulation. In: Roos, J., Costa, L. (eds.) Scientific Computing in Electrical Engineering, *Mathematics in Industry*, vol. 14, pp. 131–142. Springer, Berlin (2010)
7. Dautbegovic, E., Condon, M., Brennan, C.: An efficient nonlinear circuit simulation technique. IEEE Trans. Microw. Theor. Tech. **53**, 548–555 (2005)

8. Soveiko, N., Gad, E., Nakhla, M.: A wavelet-based approach for steady-state analysis of nonlinear circuits with widely separated time scales. IEEE Microw. Wireless Compon. Lett. **17**, 451–453 (2007)
9. Zhou, D., Cai, W.: A fast wavelet collocation method for high-speed circuit simulation. IEEE Trans. Circ. Syst. **46**, 920–930 (1999)
10. Zhou, D., Cai, W.: A fast wavelet collocation method for high-speed circuit simulation. IEEE Trans. Circ. Syst. I: Fund. Theor. Appl. **46**, 920–930 (1999)

Structural Characterization of Circuit Configurations with Undamped Oscillations

Ricardo Riaza and Caren Tischendorf

Abstract Undamped oscillations in linear circuits arise from the existence of purely imaginary eigenvalues (PIEs) in the matrix pencil spectrum which characterizes the circuit dynamics. We investigate here the circuit configurations which yield purely imaginary eigenvalues for all values of the capacitances and inductances in strictly passive problems. Our analysis is based on the use of branch-oriented circuit models and on several results from digraph theory.

1 Introduction

This communication extends our previous research on qualitative aspects of electrical and electronic circuits [7, 8] by elaborating on the so-called *hyperbolicity problem*. A circuit composed of independent voltage and current sources, and linear time-invariant resistors, inductors, and capacitors is said to be *hyperbolic* if all the eigenvalues in the spectrum are away from the imaginary axis [8]; this is a standard concept in dynamical systems theory. Linear time-invariant circuits displaying purely imaginary eigenvalues (PIEs) are important for two main reasons: on the one hand, they are responsible for undamped oscillations in linear cases and, on the other hand, when a linear circuit describes the linearization of a nonlinear one, the existence of PIEs may be responsible for Hopf bifurcations in the nonlinear problem, which in turn generate nonlinear oscillations. Our present goal is to discuss

R. Riaza (✉)
Depto. Matemática Aplicada TTI, ETSI Telecomunicación, Universidad Politécnica de Madrid, Ciudad Universitaria s/n, 28040 Madrid, Spain
e-mail: ricardo.riaza@upm.es

C. Tischendorf
Mathematisches Institut, Universität zu Köln, Weyertal 86-90, 50931 Köln, Germany
e-mail: tischendorf@math.uni-koeln.de

M. Günther et al. (eds.), *Progress in Industrial Mathematics at ECMI 2010*, Mathematics in Industry 17, DOI 10.1007/978-3-642-25100-9_2,

a full characterization of the configurations which lead to purely imaginary eigenvalues for all positive values of the capacitances and inductances involved in the circuit.

Current approaches to circuit analysis in the time-domain make systematic use of models based on differential-algebraic equations (DAEs) (see e.g. [1–3, 5, 6, 9, 10]). Background material on the DAE circuit models to be used is given in Sect. 2. The attention will be focused on so-called branch-oriented models. In Sect. 3 we characterize the circuit configurations which yield PIEs for all reactive values, the graph-theoretic notion of a *P-structure* being the key element in our analysis. Finally, Sect. 4 comprises some concluding remarks.

2 Circuit Model

A linear electrical circuit defined by resistors, capacitors, inductors, and independent voltage and current sources can be modelled by means of the DAE

$$C v_c' = i_c \tag{1a}$$

$$L i_l' = v_l \tag{1b}$$

$$0 = B_c v_c + B_l v_l + B_r v_r + B_j v_j + B_u v_s(t) \tag{1c}$$

$$0 = Q_c i_c + Q_l i_l + Q_r i_r + Q_j i_s(t) + Q_u i_u \tag{1d}$$

$$0 = i_r - G v_r. \tag{1e}$$

We split the vectors of (capacitor, inductor, resistor, current and voltage sources) branch voltages and currents as $v = (v_c, v_l, v_r, v_j, v_s(t))$ and $i = (i_c, i_l, i_r, i_s(t), i_u)$. Equations (1c) and (1d) express in matrix form Kirchhoff's voltage and current laws, making use of the reduced loop and cutset matrices $B = (B_c \;\; B_l \;\; B_r \;\; B_j \;\; B_u)$, $Q = (Q_c \;\; Q_l \;\; Q_r \;\; Q_j \;\; Q_u)$. Further details on these models can be found in [4, 6]. We will assume throughout the paper that the capacitance and inductance matrices C and L are diagonal with positive entries, and that the conductance matrix G is positive definite. Hence, all devices are linear and strictly passive, and capacitors and inductors are uncoupled. Additionally, the circuits will have neither IC-cutsets (that is, cutsets formed just by current sources and/or capacitors) nor VL-loops (namely, loops defined by voltage sources and/or inductors only).

The eigenvalue analysis can be simplified by working with the so-called *reduced* circuit obtained after open-circuiting current sources and short-circuiting voltage sources (cf. [8]). We will hence look for values of λ of the form $\pm\alpha j$, with $\alpha \in \mathbb{R} - \{0\}$ (and $j = \sqrt{-1}$), yielding non-trivial solutions for the linear system

$$\lambda C v_c = i_c \tag{2a}$$

$$\lambda L i_l = v_l \tag{2b}$$

$$B_c v_c + B_l v_l + B_r v_r = 0 \tag{2c}$$

$$Q_c i_c + Q_l i_l + Q_r i_r = 0 \tag{2d}$$

$$i_r = G v_r. \tag{2e}$$

Besides standard properties of digraphs [6,8] we will need the concept of a *block*.

Definition 1. A node is said to be an *articulation* if the removal of it and its incident branches increases the number of connected components of the digraph. A digraph is said to be *non-separable* if it is connected and has no articulations. A *block* is a maximal non-separable subgraph.

For our purposes, the main property of blocks is the fact that the branches of a block do not belong to any loop or cutset including branches from outside the block. Given a distinguished set of branches K, we will call a loop or cutset including elements from both K and $G-K$ a *hybrid* loop or cutset, respectively. The branches of a block K do not take part either in hybrid loops or in hybrid cutsets.

3 Purely Imaginary Eigenvalues

We will make use of some previous results detailed in [8]. Specifically, the circuit pencil is known to have a zero eigenvalue if and only if the circuit has at least one IC-cutset or one VL-loop; we preclude these configurations in order to focus the hyperbolicity analysis on the existence of non-zero, purely imaginary eigenvalues. We also know from [8] that eigenvectors associated with purely imaginary eigenvalues must necessarily have vanishing voltage and current in the resistor branches.

Additionally, a well-known property in circuit theory states that all eigenvalues of an LC-circuit are purely imaginary. Hence, if after open-circuiting current sources and short-circuiting voltage sources in a VIRLC circuit there exists an LC-block, then the spectrum includes a PIE. The converse is not true, however; counterexamples can be found in [8], where certain strictly passive RLC circuits without LC-blocks are shown to exhibit PIEs for certain values of the reactances. However, a natural conjecture says that if a circuit has PIEs for *all* positive values of the reactances, it must be because an LC-block shows up after open-circuiting current sources and short-circuiting voltage sources. This is actually true, as stated below.

Theorem 1. *A linear, time-invariant circuit has a pair of purely imaginary eigenvalues for all positive values of capacitances and inductances if and only if there exists an LC-block in the circuit obtained after open-circuiting current sources and short-circuiting voltage sources.*

The proof proceeds via the notion of a *P-structure* as introduced below. In what follows we work with the reduced RLC circuit without further explicit mention.

In view of the identities $v_r = i_r = 0$ holding true for PIEs, the eigenvalue-eigenvector equations (2) read

$$\lambda C v_c = i_c \tag{3a}$$

$$\lambda L i_l = v_l \tag{3b}$$

$$B_c v_c + B_l v_l = 0 \tag{3c}$$

$$Q_c i_c + Q_l i_l = 0, \tag{3d}$$

for which a solution $\lambda = \alpha j \neq 0$ is assumed to exist for all positive values of C and L. Needless to say, the actual values of λ and α will depend on C, L. Fix a set of values for C and L, and focus on the non-vanishing entries of v_c, v_l, i_c and i_l within an associated eigenvector. Note that, from (3a) and (3b), exactly the same entries vanish in the voltage and the current vector. Additionally, not all v_l's (hence not all i_l's) can vanish since, otherwise, the equation $B_c v_c = 0$ resulting from (3c) would indicate the existence of a C-cutset. Analogously, not all i_c's (hence not all v_c's) may vanish since $Q_l i_l = 0$ from (3d) would signal an L-loop.

Denote by K the set of capacitive and inductive branches with non-vanishing voltage and current in the above-referred eigenvector. We will use the subscript k to denote the corresponding (non-vanishing) entries of v_c, v_l, i_c and i_l, and also to specify the submatrices of B_c, B_l, Q_c and Q_l defined by the columns which correspond to K-branches, as well as the capacitances and inductances of the K-branches. This makes it possible to recast (3) as

$$\lambda C_k v_{ck} = i_{ck} \tag{4a}$$

$$\lambda L_k i_{lk} = v_{lk} \tag{4b}$$

$$B_{ck} v_{ck} + B_{lk} v_{lk} = 0 \tag{4c}$$

$$Q_{ck} i_{ck} + Q_{lk} i_{lk} = 0. \tag{4d}$$

Note that every K-branch forms at least one cutset just with other K-branches, as a consequence of the fact that all v_{ck} and v_{lk} in (4c) do not vanish. Indeed, since $(v_{ck}, v_{lk}) \in \ker (B_{ck} \; B_{lk})$, this vector can be written as a linear combination of vectors describing K-cutsets; additionally, every K-branch must have a non-vanishing entry in at least one of these vectors since, otherwise, the corresponding entry in v_{ck} or v_{lk} would vanish. Proceeding analogously, (4d) indicates that every K-branch forms at least one loop just with other K-branches. This motivates the following definition.

Definition 2. A set K of capacitive and inductive branches, together with their incident nodes, is said to form a *P-structure* if every branch in K forms at least one cutset and at least one loop just with other branches from K.

Here the cutset and the loop need not include all the branches in K; nor it must happen that the cutset and the loop involve the same branches. For the sake of

terminological simplicity we will use K also to mean the subgraph defined by the K-branches and their incident nodes. P-structures are the candidates which may (but not necessarily do) support the existence of a PIE. In the light of Definition 2, the discussion above indicates that the branches corresponding to the non-vanishing entries of an eigenvector associated with a PIE form a P-structure.

Now, an LC-block which does not amount to a single branch can be checked to be a P-structure (note, incidentally, that the P-structures from which a PIE-eigenvector arises include at least two branches, namely a capacitor and an inductor). Certainly, the converse is not true. The proof of Theorem 1 will be closely related to this fact.

Fix an eigenvector associated with a PIE, to be denoted by (v_c, v_l, i_c, i_l), and consider the associated P-structure K signaled by its non-vanishing entries. Let b_k, n_k and c_k stand for the number of branches, nodes and connected components of K.

Lemma 1. *If the P-structure K is not a block, then the rank of $B_k = (B_{ck}\ B_{lk})$ is greater than $b_k - n_k + c_k$; if it is a block then* $\mathrm{rk}\, B_k = b_k - n_k + c_k$.

Indeed, K defines a subgraph and therefore its cycle space has dimension $b_k - n_k + c_k$. This implies that there exist $b_k - n_k + c_k$ linearly independent K-loops, which are loops of the original digraph. If K is a block, then the absence of hybrid loops and cutsets easily yields $\mathrm{rk}\, B_k = b_k - n_k + c_k$. By contrast, if it is not a block, it can be shown that there must exist a hybrid loop; its K-entries cannot be expressed in terms of those corresponding to the $b_k - n_k + c_k$ K-loops mentioned above, meaning that in this case the rank of B_k must be greater than $b_k - n_k + c_k$.

According to Lemma 1, the first $b_k - n_k + c_k$ rows of (4c) read $\tilde{B}_k v_k = 0$, where v_k stands for (v_{ck}, v_{lk}). In turn, regarding the cutset matrix Q, notice that $\ker Q_k$ is spanned by linearly independent K-loops. Since the K-loops are the same in the original circuit and in the K-subcircuit, this means that $\ker Q_k$ equals $\ker \tilde{Q}_k$, where $\tilde{Q}_k$ is any (reduced) cutset matrix of the K-circuit. This means that (4d) can be recast as $\tilde{Q}_k i_k = 0$, i_k standing for (i_{ck}, i_{lk}). The next result follows from these remarks.

Lemma 2. *A PIE of the original circuit is also a PIE of the corresponding K-subcircuit, the non-vanishing entries of the original eigenvector defining an eigenvector of the K-subcircuit.*

Proof of Theorem 1. Our reasoning is supported on the fact that all PIE-eigenvectors must arise from some P-structure, according to Lemma 2. Consider a P-structure K, and choose the values of capacitances and inductances of the K-subcircuit in such a way that all eigenvalues of that subcircuit are simple. This can be done for parameter values lying on an open dense subset in $\mathbb{R}_+^{b_k}$, where b_k is the number of branches in K and $\mathbb{R}_+$ is the set of positive real numbers, as a consequence of the fact that eigenvalues are given by the roots of the pencil determinantal polynomial, which has the form $p(\lambda, C, L) = a_m(C, L)\lambda^m + \ldots + a_0(C, L)$. Note that $a_0(C, L) \neq 0$ because the absence of C-cutsets and L-loops rules out null eigenvalues. Multiple eigenvalues are defined by the intersection of $p(\lambda, C, L) = 0$ and $\partial p/\partial\lambda(\lambda, C, L) = 0$ and, therefore, occur only on a lower dimensional set of the parameter space. This means that the set of values of C_k, L_k for which all